# APPENDIX A
# INFORMATION PERTAINING TO IMAGE PROCESSING

## A.1 List of light sources and their suitable applications

1. *Daylight* is generally not suitable for image processing because both light intensity and colour depend highly on the time of day and weather conditions.
2. *Fluorescent lamps* produce a large homogeneous illumination field and do not get hot. Frequency rectifiers can be easily implemented to prevent modulation of the light intensity and frequency interference. However, there is a spectral limitation associated with the tube-fill that results in low intensity of the illumination field.
3. *Tungsten light sources* are inexpensive but are not well suited for image processing because the light intensity varies over the period of the frequency of the alternating current. This is especially the case when the camera frame rate is not a multiple of the current frequency, resulting in interference and loss of image quality. This disadvantage can be overcome by using a direct current power source. There are however further disadvantages associated with tungsten light sources as they produce a non-uniform illumination field and can get very hot.
4. *Quartz Tungsten Halogen (QTH) lamps* eliminate the problems associated with alternating current frequency. Like normal tungsten lamps, QTH lamps have a tungsten filament inside the bulb that glows when connected to electricity. However the bulb is filled with a small amount of halogen (iodine or bromine compounds) and a gas. When the lamp is turned on the tungsten atoms are emitted from the hot filament (3300°C) and cool down to less than 1400°C. At this temperature the tungsten atoms react chemically with the halogen atoms, forming a compound that is gaseous at temperatures above 250°C. The thermal current of the halogen gas carries the compound molecules back towards the hot tungsten element where the high temperature causes them to breakdown into their constituents (tungsten and halogen). The halogen is freed and the tungsten reattaches to the filament and the process starts again. This continuous rejuvenation of the tungsten filament allows the filament temperature to be much

higher than that of a normal tungsten lamp and also results in almost constant light intensity over the period of the alternating current.

5. *Discharge lamps* provide a constant illumination field and have high radiation densities. They are generally used for strobed illumination and are relatively expensive.
6. *Light emitting diodes (LED's)* have excellent light intensity control over a wide range of wavelengths and are inexpensive. They are quick to respond to an input signal, making them ideal for strobing applications. Applications generally require multiple diodes arranged in arrays or as a ring light.
7. *Lasers* involve focusing high radiation density light over a small area and hence laser light is very chromatic and consistent.
8. *Infrared light sources* are employed in scenarios where elimination of daylight and other light sources is otherwise impossible.

### A.2 Methods of lighting a subject

There are four methods of illuminating a subject, and these are most easily categorised by the relative positions of the camera and the chosen light source.

1. *Incident light illumination:* The camera and light source are positioned on the same side of the subject, with the light projected on the subject at some suitable incident angle. The image displays the light reflected by the subject, and this method is thus suitable for showing objects as they physically appear.
2. *Light-field illumination:* Camera and light source are positioned on the same side of the subject. The light is projected along the camera axis and the subject reflects the light directly back at the camera. Light-field illumination is suited to showing dark objects against a light background.
3. *Dark-field illumination:* As with light-field illumination, the camera and light source are positioned on the same side of the subject. The light is projected at a sufficiently small incident angle so that the camera only captures the scattered light from the subject. Dark field illumination will lighten an object and darken the image background.
4. *Transmitted light illumination:* The light source is positioned on the opposite side of the object to the camera. The resulting image shows the subject as a dark object on a light background.

## A.3 CCD sensor architectures

Following Ehrdt–Ferron (2000), the three principal methods of integrating CCD pixel information into a serial data stream are as follows.

1. *Interline transfer sensors* (are subdivided into light sensitive and storage regions that are arranged in alternating columns as shown in Figure A.1(a). Electron charges are integrated in the light sensitive cells and quickly transferred into the storage cells. The data is then transferred into the horizontal output register one line at a time and output to the video input unit. Because both the connectors between cells and the storage cells are not sensitive to light, the portion of the sensor that is light sensitive is relatively small. Hence, interline transfer sensors are much less light sensitive than frame and full-frame transfer sensors. However, lens-on-chip technology reduces this disadvantage by providing each sensor cell with a micro-lens that offsets the light falling on the storage region onto the light sensitive region of the sensor cell. This can result in a sensitivity increase of up to 100%.
2. *Frame transfer sensors* (Figure A.1(b)) separate the light sensitive and storage areas into two blocks. Hence the total sensor area is approximately twice that of an interline transfer sensor. The total charge received by the light sensitive region is transported into the storage region and then into the horizontal output register one line at a time.
3. *Full frame transfer sensors* (Figure A.1(c)) do not involve a storage area. Hence the entire sensor area is light sensitive. After the pixel data is integrated, the camera shutter is closed and the data is transferred directly to the output register one line at a time. It is a requirement of the full frame architecture that the camera has a shutter. The full frame CCD architecture makes for very fast data transfer rates and hence this arrangement is used in most time-critical applications.

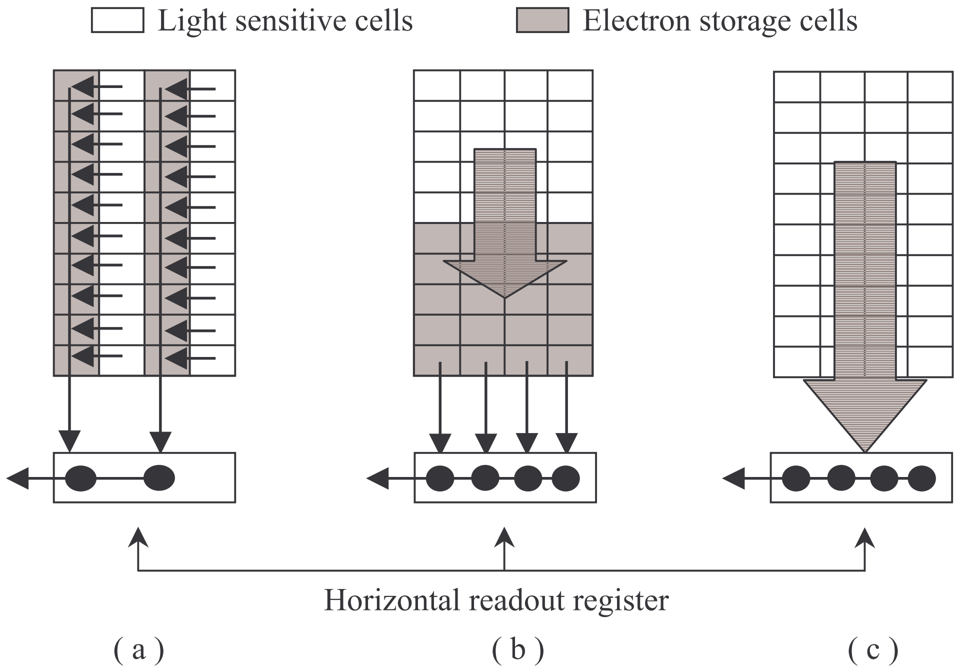


Figure A.1. CCD Sensor architectures: (a) Interline transfer, (b) Frame transfer, and (c) Full frame transfer architectures.

The above description of CCD sensor architecture relates to monochrome area scan cameras, that generally employ a single two–dimensional 4:3 matrix of CCD pixels. Colour cameras however, produce an image that consists of three distinct parts; red, green and blue (RGB). Almost any colour can be produced by additive colour mixture of these three colours. Two distinctive types of colour camera formats are available.

1. *Single chip colour cameras* separate the incoming light into its three parts using either a mosaic or stripe filter that is located directly on the CCD sensor. Each filter stripe or elements of the mosaic is transparent to only one of the RGB colours respectively. Pixels of the red, green and blue sections are read out successively and electronic switches are employed to divide the signal into these three primary colours. This method of filtering reduces the image resolution by a factor of 2 in two dimensions (mosaic filter) or a factor of 3 in one dimension (stripe filter) as can be seen in Figure A.2.

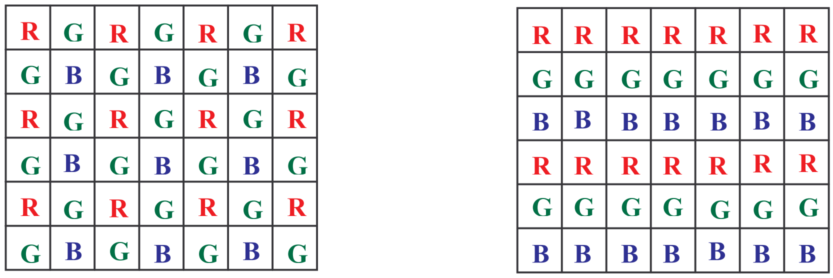


(a) (b)

Figure A.2. Single chip CCD colour production: (a) Mosaic filter, (b) Stripe filter.

2. *Three chip colour cameras* employ separate CCD sensors for each of the three RGB colours. Prisms located in the path of incoming light separate the light into the RGB components and direct each component to the appropriate CCD sensor (Figure A.3). The read–out from each of these three sensors are stored in different areas of the image RAM and can hence be dealt with separately. There is no loss of resolution between a monochrome camera and a three CCD colour camera.

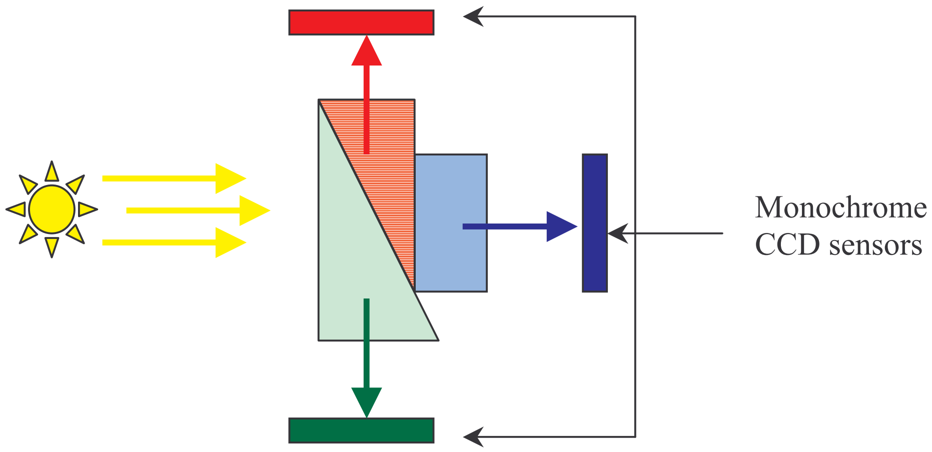


Figure A.3. Three chip colour camera arrangement showing prismatic separation of incoming light into its RGB components.

### A.4 Geometric principles of lenses

Consider light rays from an object at some distance from a CCD camera. As this distance approaches infinity, the light rays become parallel (Figure A.4(a)). A lens positioned perpendicular to these light rays will refract, converge and focus this incoming light at the focal point (f) of the lens. Hence the focal point of a lens is defined by its physical geometry. In order for a CCD sensor to collect a focused image of this object, it would have to be positioned at the focal point. The distance between the lens and the focal point is referred to as the focal length ($L_f$).

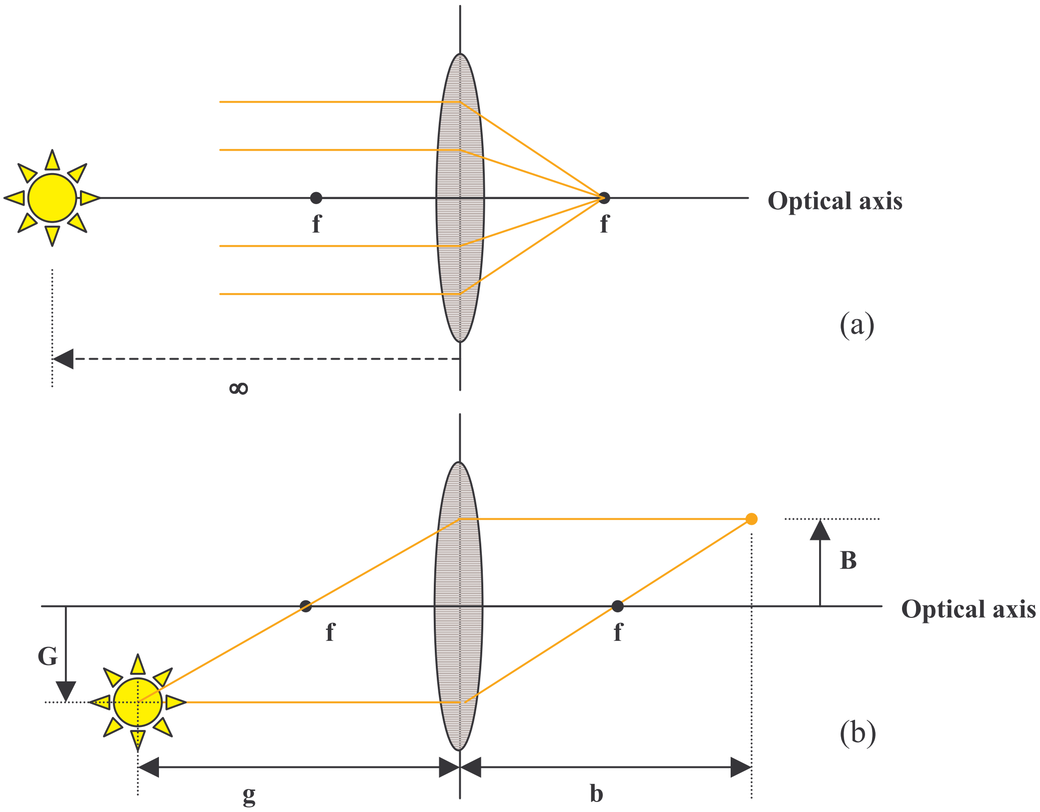


Figure A.4. Geometric principle of a thin lens: a) Object located at infinite distance, resulting in an image focused on the focal point (f); b) Object positioned at finite distance (g,G) from the lens, resulting in a focused image behind the focal point at (b,B).

In reality, most objects reflecting light are located at a finite axial distance (g) from the lens (Figure A.4(b)). The lens will focus the incoming light from this object onto a point behind the focal point. For a CCD sensor to collect the image, the distance between the CCD and the lens must be increased accordingly. The object distance, image distance and focal length can be related with simple trigonometry in what might be considered a thin-lens idealisation, as lens aberrations are neglected. This assumption is valid for optical calculations for modern lens, which incorporate precision manufacture and refractive correction. Hence:

$$\frac{1}{g} + \frac{1}{b} = \frac{1}{L_{\mathbf{f}}} \qquad \text{(EQ A.1)}$$

The aspect ratio of the system $(m)$ is thus easily deduced.

$$m = \frac{b}{g} = \frac{B}{G} \qquad \text{(EQ A.2)}$$

Hence, the image and object distances can be determined for a lens with known focal length:

$$b = L_{\mathbf{f}}(1 + m) \qquad \text{(EQ A.3)}$$

$$g = L_{\mathbf{f}}(1 + \frac{1}{m}) \qquad \text{(EQ A.4)}$$

Hence, focusing of a CCD camera can be thought of as simply adjusting the distance between the CCD sensor system and the camera lens. For any lens it is possible to determine the minimum object distance $(g_{\text{min}})$ for focusing, by considering the maximum available distance between the lens and CCD ($b = b_{\text{max}}$). Hence:

$$g_{\text{min}} = \frac{L_{\mathbf{f}} \cdot b_{\text{max}}}{b_{\text{max}} - L_{\mathbf{f}}} \qquad \text{(EQ A.5)}$$

It is important to note the availability of spacer rings, which can be placed between the lens and the CCD sensor system in order to increase the magnitude of $b_{\text{max}}$.
For a specific image processing application, an estimate of the required lens focal length can be calculated as follows:

$$L_{\mathbf{f}} = \frac{m \cdot g}{1 + m} = \frac{b}{1 + m} \qquad \text{(EQ A.6)}$$

The photographic angle (υ) is another important characteristic of a lens (Figure A.5). The upper limit of (υ) is dependent upon the focal distance of the lens and the diagonal dimension of the CCD sensor. Hence,

$$\upsilon = 2\arctan\left(\frac{B_{\max}}{2L_{\mathrm{f}}}\right) \qquad \text{(EQ A.7)}$$

where ($B_{\max}$) is the maximum (diagonal) dimension of the CCD chip capturing the image.

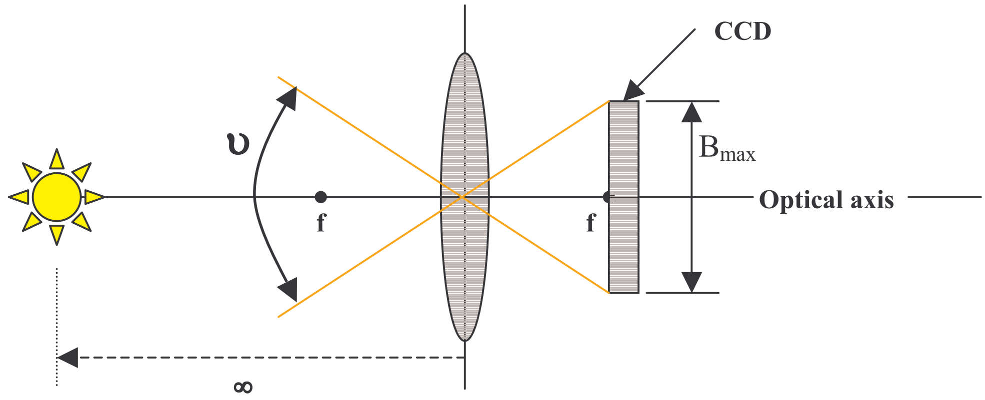


Figure A.5. Lens system illustrating the photographic angle (υ).

The depth of field (d) refers to the distance either side of the object plane at (g) that will appear focused on the image of the object plane. This concept is illustrated in Figure A.6.

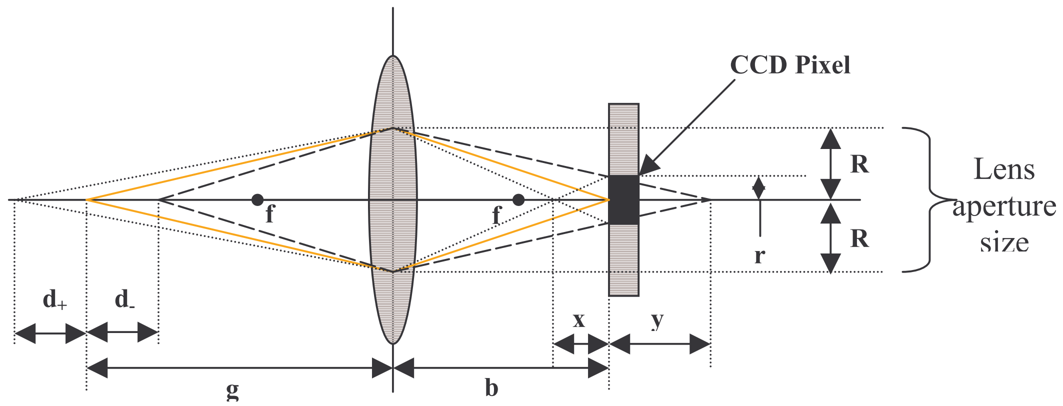


Figure A.6. Lens depth of field geometry.

Figure A.6 shows that an object located within the domain ($d = d_+ + d_-$) will be clearly defined in the resulting image. As mentioned previously, the depth of field is inversely proportional to and hence dependent upon the size of the lens aperture (2R). Following thin lens theory (Cutnell and Johnson 1998), the size of a lens aperture is commonly measured in **f**_stops and is simply the ratio of the focal length and aperture diameter.

$$\mathbf{f}\_stops = \frac{L_{\mathbf{f}}}{2R} \quad \text{(EQ A.8)}$$

The camera uses the inverse of this **f**_stops value as a measure of the environment light intensity.

# APPENDIX B
# NUMERICAL IMAGE MASKING ROUTINES

## B.1 Flat-platen confined uniaxial compression

For the situation of flat-platen confined uniaxial compression, stationary cell and platen surfaces visible in the image are masked based on the four corner points of the sample in the image, as shown in Figure B.1.

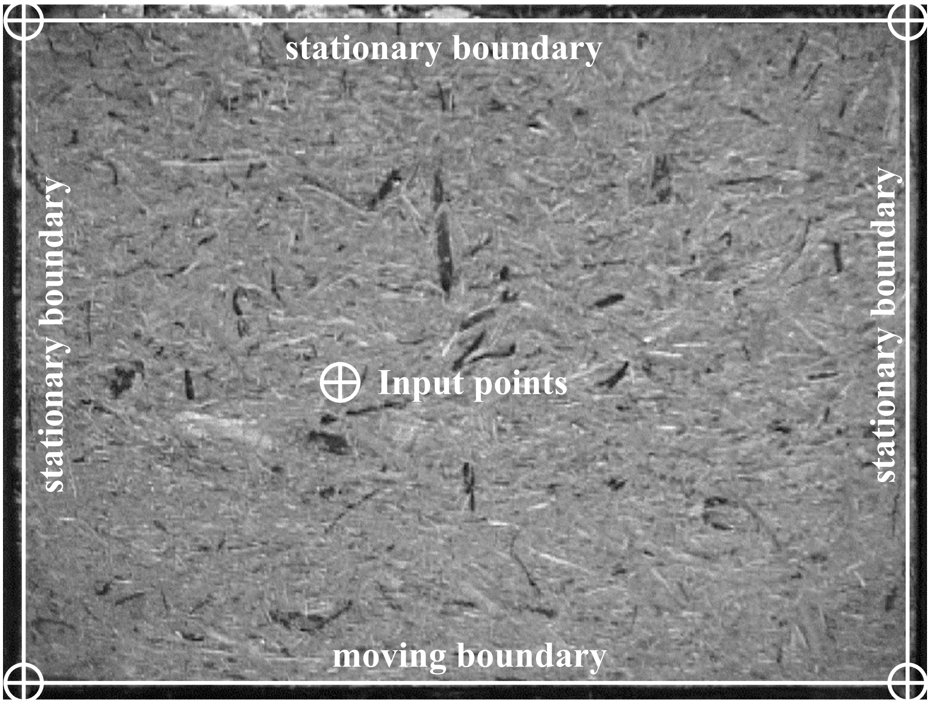


Figure B.1. Flat platen uniaxial masking parameters.

The moving platen boundary is masked transiently throughout the image series. The image pixel to millimetre scale is utilised to convert the physical velocity of the moving platen to a value in pixels per second. The time increment between sequential images being masked is known and used to evaluate the pixel displacement of the platen over this time increment. Masking routines were developed to determine the transient platen displacement for both constant and sinusoidal platen paths and subsequently mask the boundaries in each image in the series.

### B.2 Grooved-platen confined uniaxial compression

For the scenario of grooved-platen confined uniaxial compression, the masking technique is the same as that for flat-platen experiments in regard to both stationary surfaces and the transient placement of the moving platen mask. However, linear functions were developed to mask the grooved surfaces accurately by defining a start point, a pixel to millimetre scale, the number of grooves to mask and the specific groove geometry (pitch, angle and landing width of the teeth). This is illustrated in Figure B.2 for a confined uniaxial compression experiment involving 25mm pitch, 35° grooving with a 3mm landing width. Grooved-platen masking routines were developed for both constant and sinusoidal platen paths.

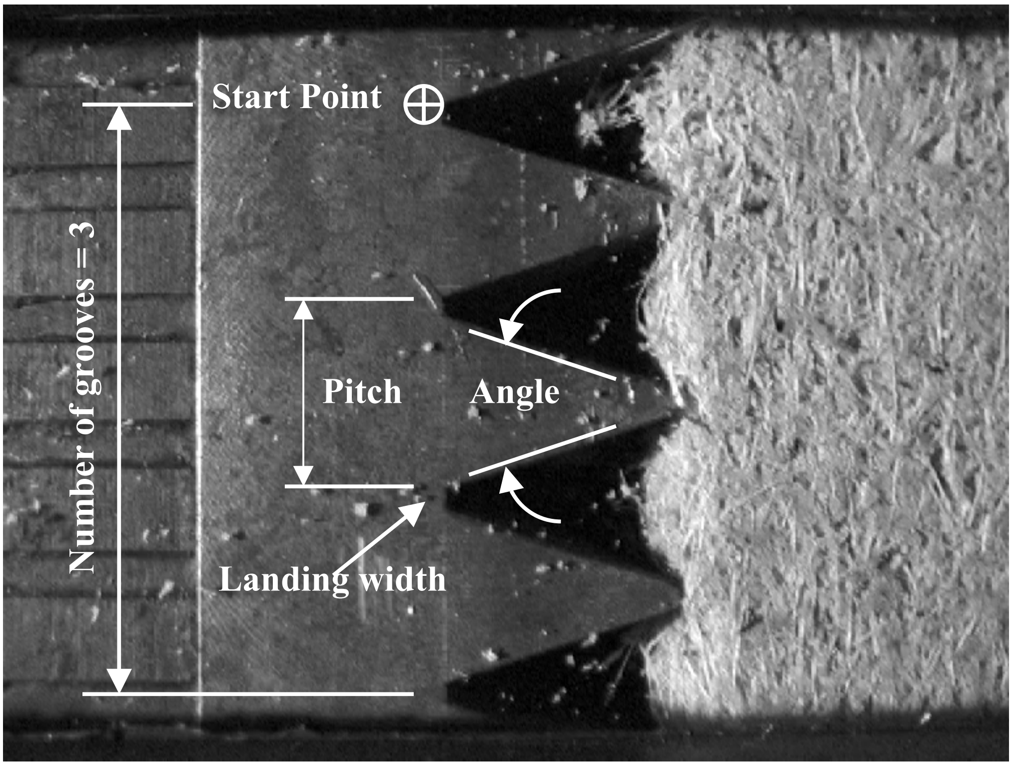


Figure B.2. Grooved platen uniaxial masking parameters.

### B.3 Flat roll two-roll milling

Masking of imagery from flat two-roll milling experiments involves input of two points on each of the two roll surface boundaries. The theoretical centre of each roll is determined based on the roll radius and a pixel to millimetre scale. With known centre points, the equations of the roll boundaries can be determined and used to identify the vertical location of the roll boundary in the image, for all horizontal pixel values occupied by the roll surface. This procedure is illustrated for the top roll in Figure B.3.

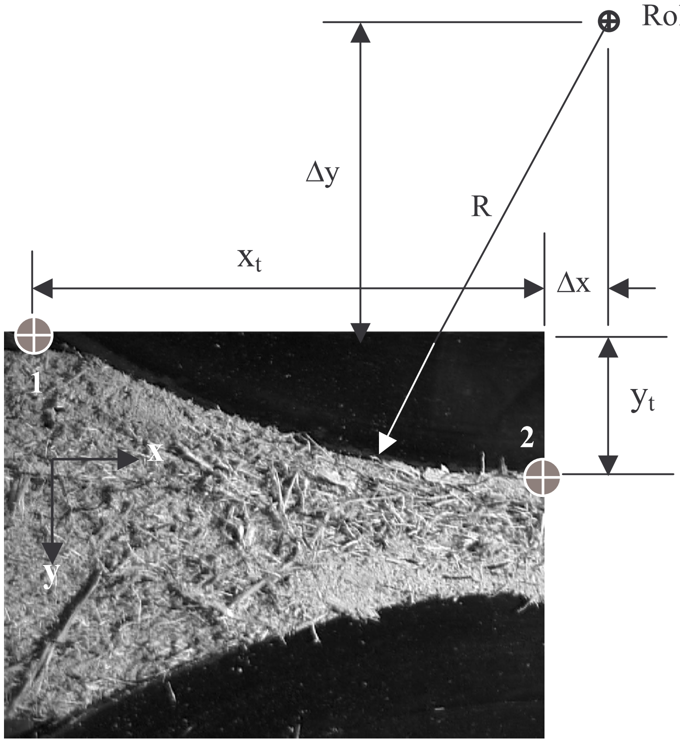


**Roll Boundary Equations**

<u>Point 1</u>
$(xt + \Delta x)^2 + (\Delta y)^2 = R^2$

<u>Point 2</u>
$(\Delta x)^2 + (yt + \Delta y)^2 = R^2$

Figure B.3. Roll surface masking method.

Simultaneous solution of the roll boundary equations at points (1) and (2) yields unique solutions for ($\Delta x$) and ($\Delta y$). The software determines these parameters and hence allows deduction of the surface location in the (y) direction for any (x) pixel value specified.

Examples of images masked with a grey–scale value of zero (white) are shown in Figure B.4.

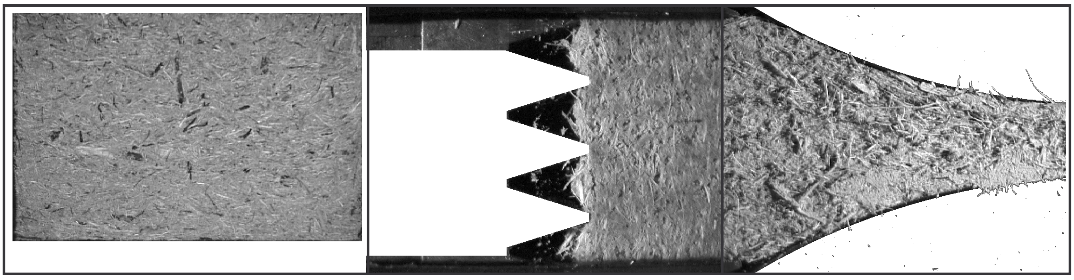

(a) (b) (c)

Figure B.4. Examples of masked images: a) Flat platen uniaxial compression; b) Grooved platen uniaxial compression; c) Two-roll milling.

# APPENDIX C

# ROLLING TRIALS LOAD AND TORQUE DATA

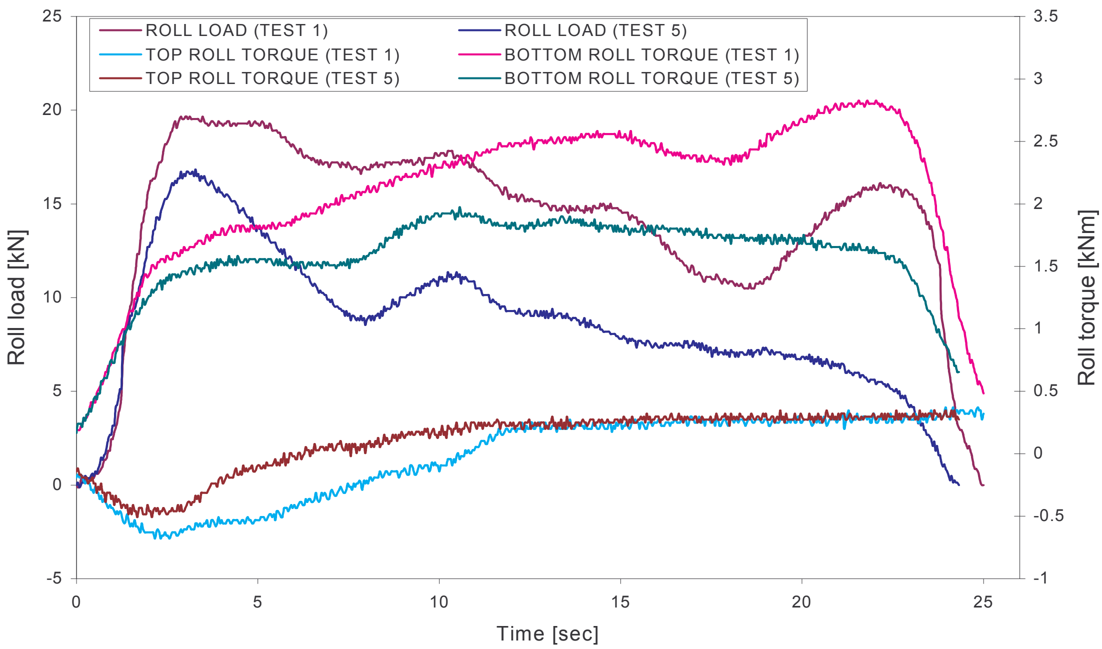


Figure C.1. Load and torque data: Test 1 and Test 5.

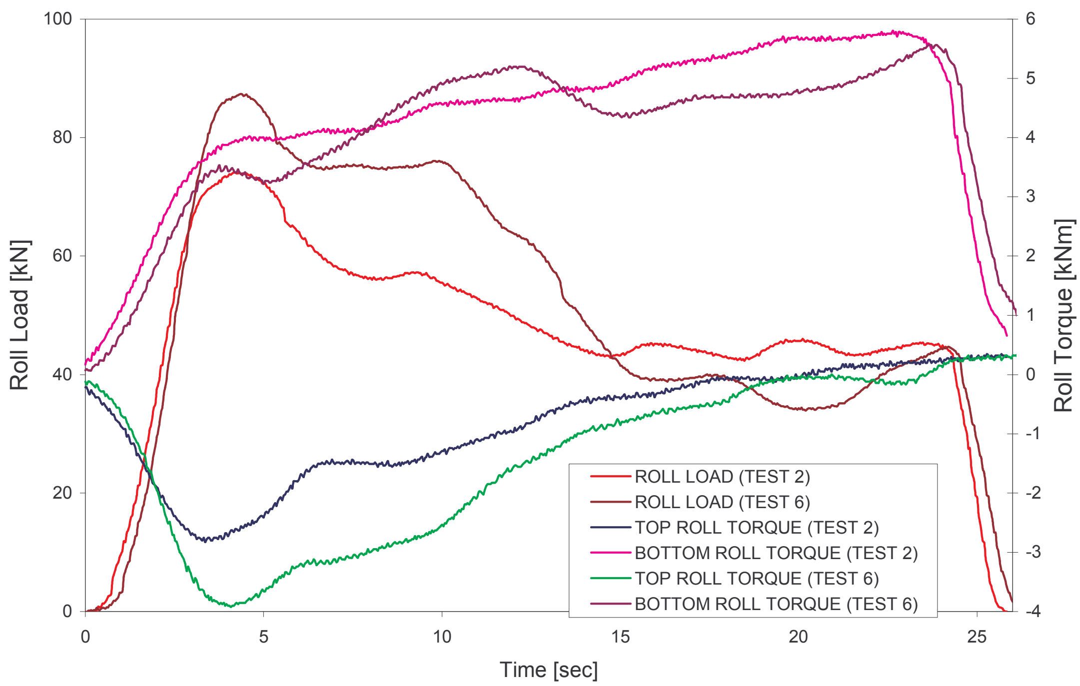


Figure C.2. Load and torque data: Test 2 and Test 6.

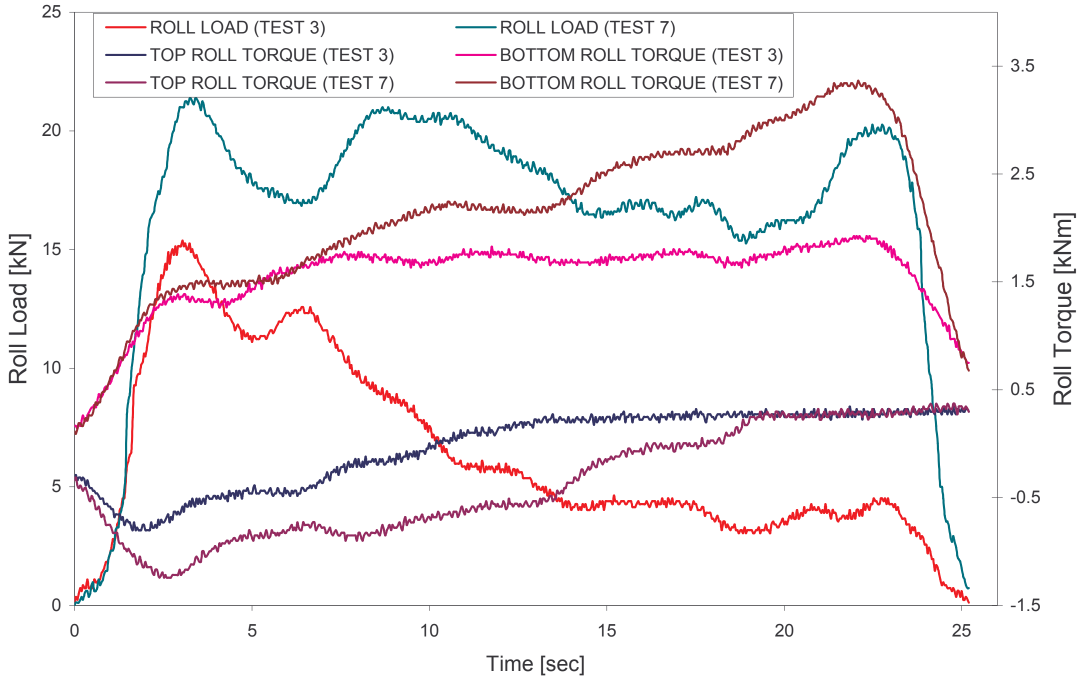


Figure C.3. Load and torque data: Test 3 and Test 7.

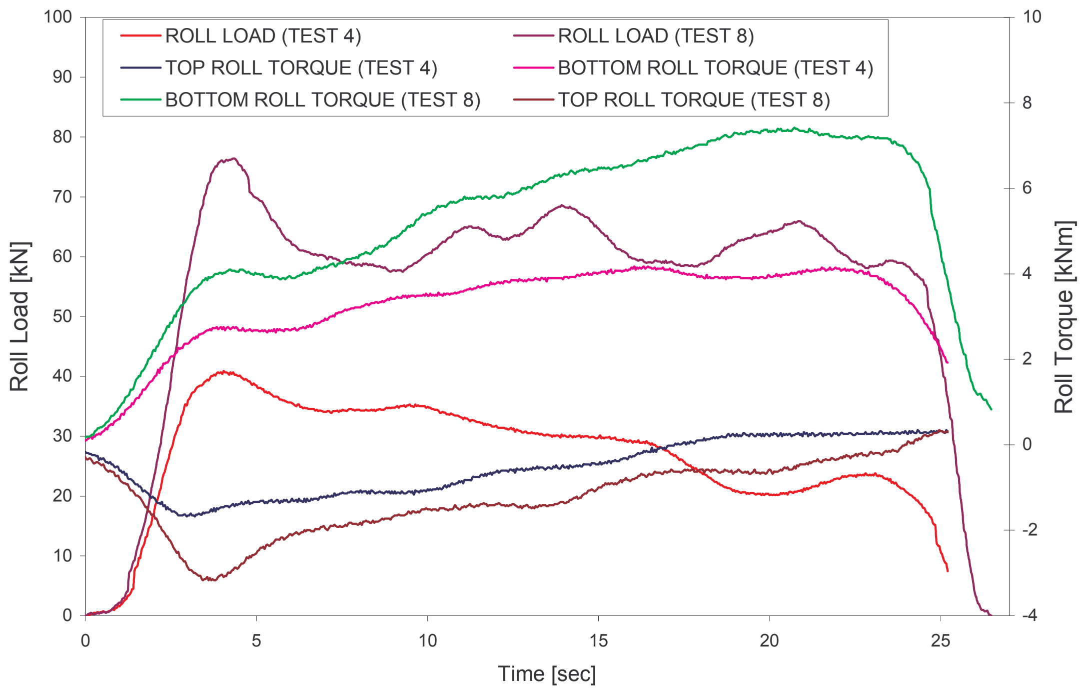


Figure C.4.  Load and torque data: Test 4 and Test 8.

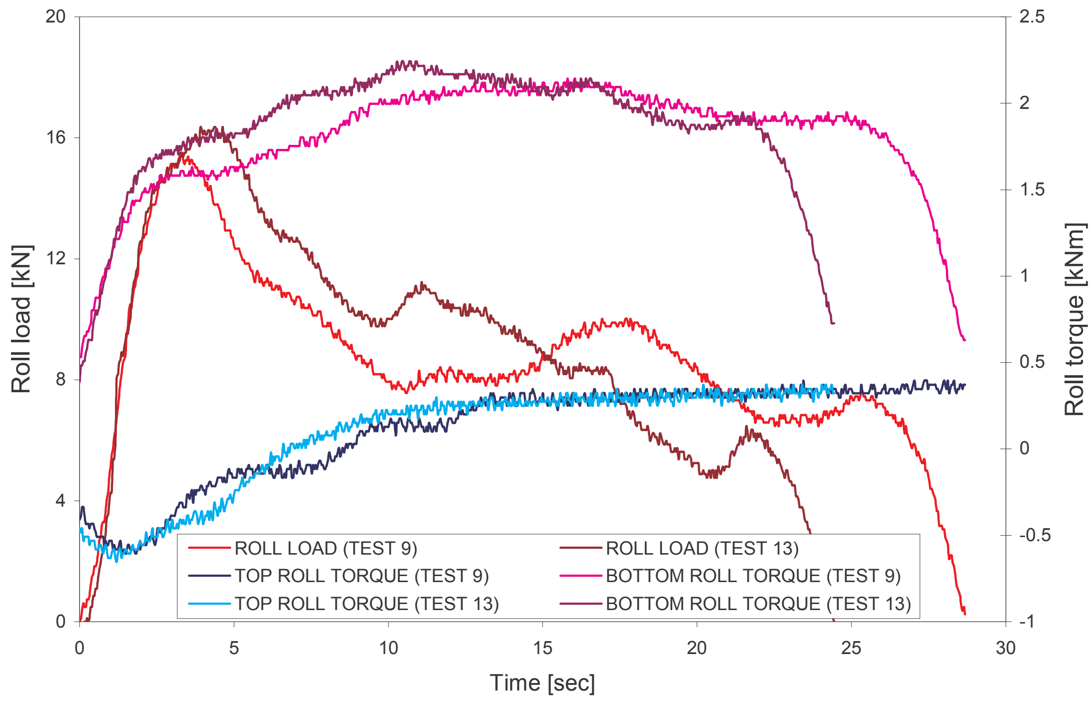


Figure C.5. Load and torque data: Test 9 and Test 13.

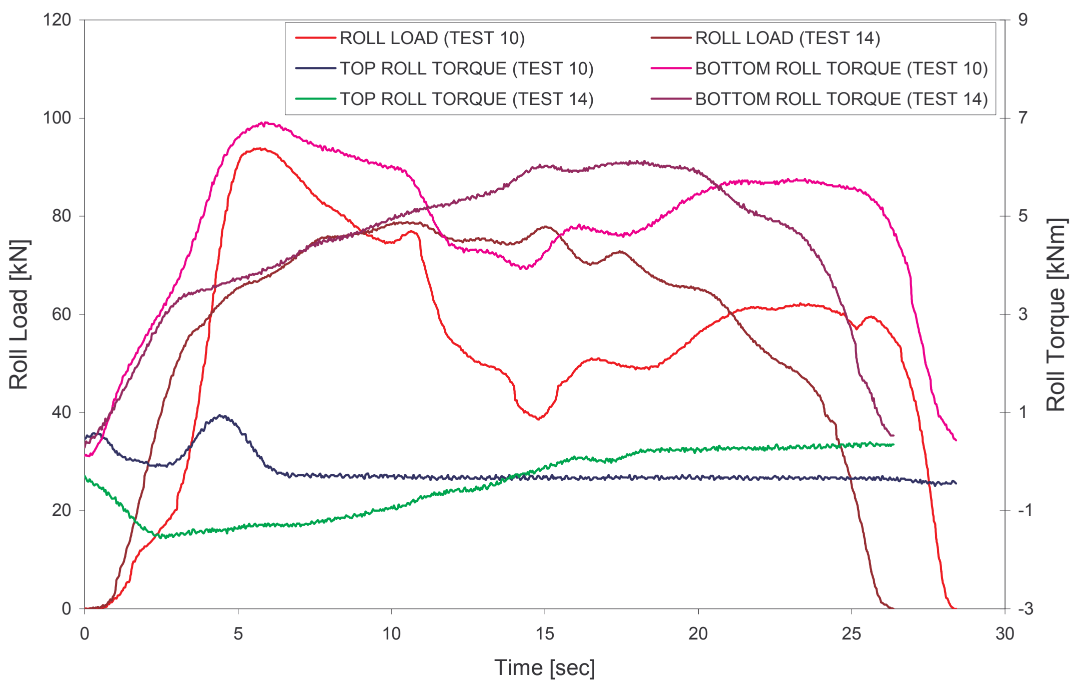


Figure C.6. Load and torque data: Test 10 and Test 14.

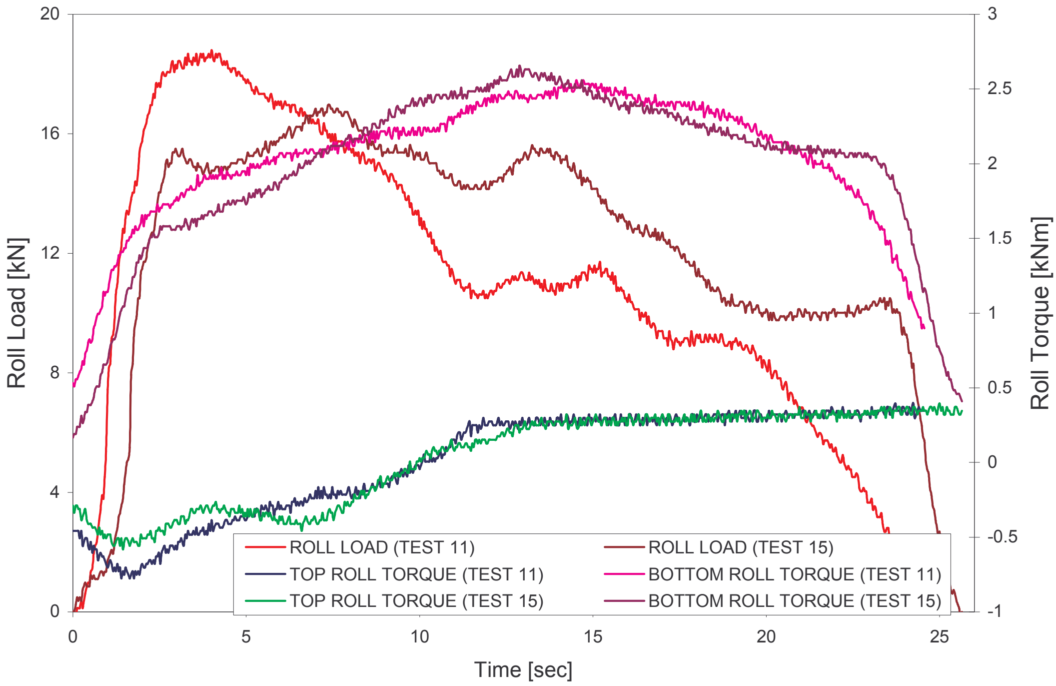


Figure C.7. Load and torque data: Test 11 and Test 15.

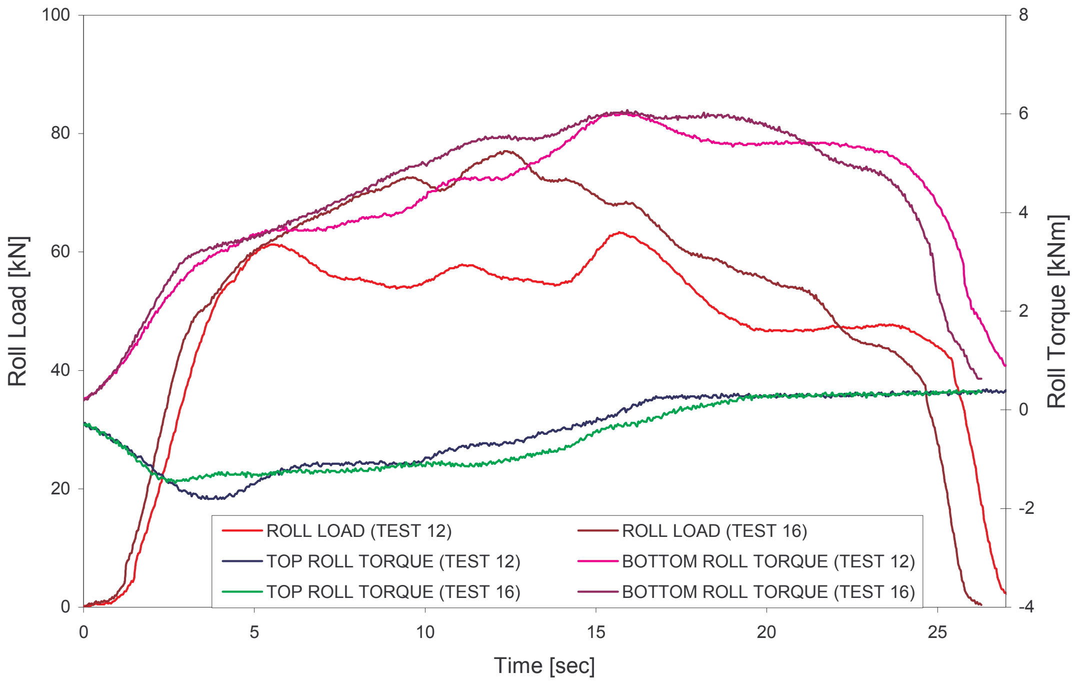


Figure C.8. Load and torque data: Test 12 and Test 16.